Exploiting the adsorption of simple gases O2 and H2 with minimal quadrupole moments for the dual gas characterization of nanoporous carbons using 2D-NLDFT models

Jacek Jagiello, Jeffrey Kenvin, Conchi Maria Concepcion Ovin Ania, José Parra, Alain Celzard, Vanessa Fierro

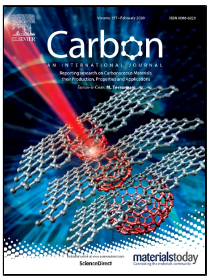

Exploiting the adsorption of simple gases O_2 and H_2 with minimal quadrupole moments for the dual gas characterization of nanoporous carbons using 2D-NLDFT models

Jacek Jagiello, Jeffrey Kenvin, Conchi O. Ania, Jose B. Parra, Alain Celzard, Vanessa Fierro

PII:	S0008-6223(20)30013-0
DOI:	https://doi.org/10.1016/j.carbon.2020.01.013
Reference:	CARBON 14947
To appear in:	*Carbon*
Received Date:	20 September 2019
Accepted Date:	03 January 2020

Please cite this article as: Jacek Jagiello, Jeffrey Kenvin, Conchi O. Ania, Jose B. Parra, Alain Celzard, Vanessa Fierro, **Exploiting the adsorption of simple gases O_2 and H_2 with minimal quadrupole moments for the dual gas characterization of nanoporous carbons using 2D-NLDFT models**, *Carbon* (2020), https://doi.org/10.1016/j.carbon.2020.01.013

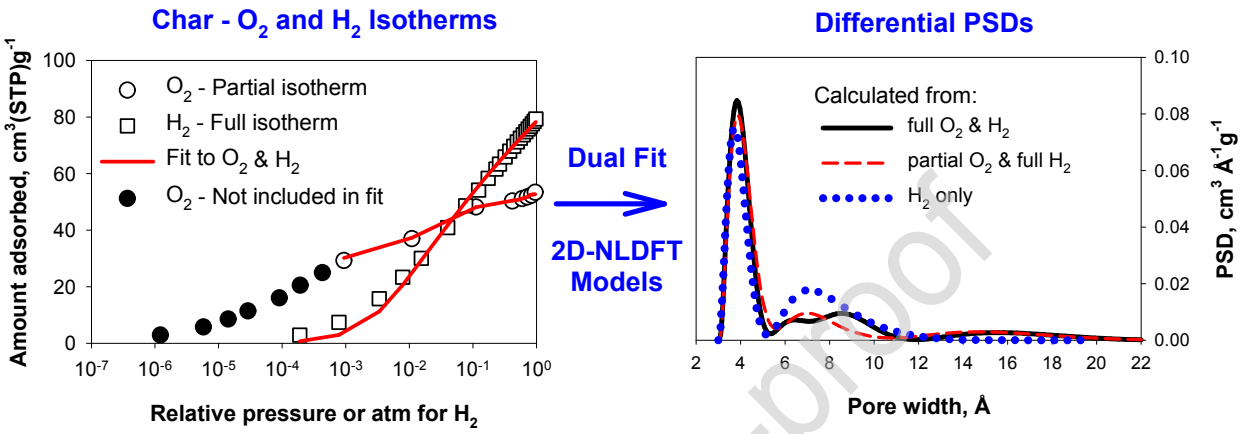

Exploiting the adsorption of simple gases O_2 and H_2 with minimal quadrupole moments for the dual gas characterization of nanoporous carbons using 2D-NLDFT models

Jacek Jagiello [a,*], Jeffrey Kenvin [a], Conchi O. Ania [b], Jose B. Parra [c], Alain Celzard [d], Vanessa Fierro [d]

[a] Micromeritics Instrument Corporation, Norcross, GA 30093, United States

[b] CEMHTI CNRS (UPR 3079), University of Orléans, 45071 Orléans, France

[c] Instituto Nacional del Carbon, CSIC, Apartado 73, 33080 Oviedo, Spain

[d] Université de Lorraine, CNRS, IJL, F-88000 Epinal, France

*Corresponding author. Tel: +1 770 624 3379. E-mail: Jacek.Jagiello@micromeritics.com

Abstract

For years, the characterization of carbon pore size distribution (PSD) has been dominated by the analysis of N_2 isotherms. Recently, the IUPAC Technical Report (2015) recommended Ar as inert gas for this analysis. N_2 molecule due to its significant quadrupole moment may selectively interact with the polar surface sites and affect the isotherm measurement. CO_2, another gas that is often used for the characterization of microporous carbons exhibits even higher quadrupole moment than N_2. In the present study, we substitute N_2 and CO_2 with O_2 and H_2 gases that have much lower quadrupole moments. The PSD calculations are performed using molecular models based on classical and quantum corrected two-dimensional nonlocal density functional theory (2D-NLDFT).

We compare the results of the dual gas analysis methods by the simultaneous fit of our models to N_2 & CO_2, and O_2 & H_2 isotherms for several reference carbon samples and demonstrate consistency between the results derived from both pairs of isotherms.

A fundamental and practical benefit of using the dual gas analysis method is the ability to obtain the full micro and mesopore PSD by using a partial O_2 isotherm without low-pressure data in combination with full H_2 isotherm both measured at 77 K.

1. Introduction

For years, the characterization of carbon pore size distribution (PSD) has been dominated by the analysis of nitrogen (N_2) isotherms measured at its boiling point (77 K). From the scientific viewpoint, however, N_2 may not be the most appropriate molecular probe for the PSD evaluation. Its high quadrupole moment may affect the adsorption of N_2 molecules due to the interactions with polar surface sites.

The molecular models used in this work for the evaluation of carbon pore structure assume nonspecific interactions of gas molecules with carbon surface. Real carbon materials may contain various mineral contaminations and chemical surface sites that may interact with adsorbate molecules via specific interactions. If the experimental adsorption isotherms are distorted by such interactions it may affect the PSDs calculated from these isotherms.

To minimize such effects IUPAC Technical Report 2015 [1] recommended argon (Ar) as the most reliable for the PSD evaluation. However, Ar adsorption measurements using liquid Ar as a coolant are more costly than the standard N_2 analysis; therefore, from the practical viewpoint, Ar analysis is not a preferred one in a typical laboratory. As a replacement for argon, it was recently proposed to use oxygen (O_2) [2]. Oxygen was chosen because its quadrupole moment has about three times lower value than N_2. Moreover, it was shown for several representative carbon samples that their PSDs derived from adsorption measurements of N_2 and O_2 at 77 K and Ar at 87 K are in quantitative agreement.

On the other hand, the Report [1] recommended using CO_2 for the characterization of ultramicroporous carbons because, at the recommended temperature (273 K), CO_2 diffuses faster into micropores than N_2 at the cryogenic temperature. This recommendation, however, is inconsistent with the premise of using molecules with low sensitivity to interactions with polar sites, because the CO_2 quadrupole moment is even larger than that of N_2, which makes it sensitive to the carbon surface chemistry [3]. In the absence of polar sites, the use of CO_2 may be appropriate, and several authors applied CO_2 adsorption to study the porosity of microporous carbons and carbon molecular sieves [4-9].

Another simple gas that diffuses faster into ultramicropores than N_2 at 77 K is H_2, which is supercritical at this temperature. Furthermore, the H_2 molecule has a small quadrupole moment and smaller diameter than CO_2, and it has been that H_2 adsorption data may provide meaningful PSD results in an extended range of pore sizes when analyzed alone [10] or simultaneously with argon data [11]. The grand canonical Monte Carlo (GCMC) model isotherms of H_2 and CO_2 were also used [12] to analyze simultaneously adsorption data of H_2 and CO_2

The values of the absolute quadrupole moments of the considered molecules are in the following order [13]: Ar <O_2 <H_2 <N_2 <CO_2 and their ratios to the value of N_2 are as follows 0.0 <0.28< 0.46 < 1.0 <3.1. Other gases such as CH_4 [14], CF_4 and SF_6 [15] with symmetrical molecules, zero quadruple moments and different molecular diameters have been used for the carbon pore size analysis as well as for the evaluation of pore connectivity and molecular sieving effects.

In present work, we use molecular models based on the nonlocal density functional theory (NLDFT) to analyze O_2 and H_2 adsorption data simultaneously. We show comparisons of PSD results derived from O_2 and H_2 data and with those from N_2 and CO_2 data. The approach introduced in this work is advantageous compared to the earlier presented "dual analysis method" [16] based on N_2 and CO_2 data, due to the lower quadrupole moments of O_2 and H_2. It is also more practically convenient because of the same cryogen, liquid N_2, used for both analyses. The PSD analysis is executed using adsorption models incorporating surface roughness, and energetic heterogeneity derived based on the NLDFT [17-20] in its two-dimensional version 2D-NLDFT-HS [21, 22] herein referred to as 2D-HS where HS stands for the heterogeneous surface.

2. Experimental

In this work, we have used two series of carbon samples derived from two precursors: (i) polyethylene terephthalate, (PET), and (ii) corn stigmata (CS). Both precursors were first carbonized to obtain chars, and then the chars were activated with CO_2. The char derived from PET was labeled PC and the activated carbons derived from this char were labeled PCn, where n is the burn-off percent during the activation process. The char derived from corn stigmata was labeled C-CS, and its two activated carbon derivatives were labeled C-CS-0.5 and C-CS-1.0, where the number in the sample label represents the time of activation in hours. Preparation and properties of the samples used in this work were described earlier for the PET series [16, 23] and the CS series [24]. In addition to the porous carbons, a sample carbon black BP 280 (Cabot) was used to obtain H_2 adsorption reference data. This carbon has been used previously [2, 21, 25] as reference for carbon material with the heterogeneous surface. The measurements of H_2 and O_2 adsorption isotherms at 77 K were performed using the high-resolution Micromeritics 3Flex instrument. The samples were degassed on sample ports at 620 K overnight before the measurements.

3. Results and Discussion

3.1 The two-dimensional NLDFT model of H_2 adsorption on heterogeneous carbon surface at 77 K

At 77 K, hydrogen is far above its critical point of 33 K and thus its adsorption isotherms on the uniform carbon surface do not show the layering transitions that lead to artifacts [21, 26] in the PSD calculations when the one-dimensional NLDFT model was applied. Nevertheless, for the evaluation of H_2 adsorption model, we use the same surface roughness parameters and type of energetic heterogeneity as in the earlier developed models for the other simple gases [2]. We calculate the kernel isotherms in the framework of the 2D-HS model [2, 21, 22] using Tarazona's version [17-19] of the non-local density functional theory (NLDFT). The theory provides a prescription for the evaluation of the density profile $\rho(\mathbf{r})$ of gas molecules confined in a pore of a given shape and dimensions. The equilibrium density profile is calculated by the iterative procedure which finds the minimum of the grand thermodynamic potential functional given by [20]

$$\Omega[\rho(\mathbf{r})] = F[\rho(\mathbf{r})] - \int d\mathbf{r}\rho(\mathbf{r})[\mu - V_{ext}(\mathbf{r})], \quad (1)$$

where F is the Helmholtz free energy functional, μ is the chemical potential, and $V_{ext}(\mathbf{r})$ is the so-called external potential which describes the pore-fluid interactions. The theoretical kernel isotherms are obtained by the integration of $\rho(\mathbf{r})$ over a pore space for a series of pressures and pore dimensions.

3.1.1 Standard slit pore model with quantum corrections

Molecular interactions of light molecules such as H_2 may be influenced by quantum effects at low temperatures. Several authors have accounted for quantum effects in modeling the adsorption of H_2 at cryogenic temperatures by using advanced simulation methods such as path integral Monte Carlo formalism [27, 28]. A simpler approach to account for quantum effects is based on the Feynman-Hibbs (FH) effective potential [29, 30]. In the present work, we apply the second-order FH effective potential that is expressed as a sum of the classical interaction potential and a quantum correction term, indicated below by the superscript "q":

$$u^{FH}(r) = u(r) + u^q(r), \quad (2)$$

where

$$u^q(r) = \frac{Q}{24}\left[\frac{d^2}{dr^2}u(r) + \frac{2}{r}\frac{d}{dr}u(r)\right] \quad (3)$$

and the composite parameter Q is given by

$$Q = (h/2\pi)^2/\mu_m k_B T \quad (4)$$

The classical interaction potential $\phi_{ff}(r)$ is assumed here in the form of the Lennard Jones (LJ) potential

$$\phi_{ff}(r) = 4\varepsilon_{ff}\left[\left(\frac{\sigma_{ff}}{r}\right)^{12} - \left(\frac{\sigma_{ff}}{r}\right)^{6}\right]. \quad (5)$$

In the above equations, r is the distance between two interacting molecules, ε_{ff} and σ_{ff} are the LJ energy and size parameters, h and k_B are the Planck and Boltzmann constants, μ_m is the reduced mass of the two interacting particles. For the interaction between the two H_2 molecules $\mu_m=m/2$, where m is the mass of the H_2 molecule. For the interaction between H_2 molecule and the solid $\mu_m=m$.

For the LJ potential Eq. (3) takes the following form

$$\phi^{q}_{ff}(r) = Q\varepsilon_{ff}r^{-2}\left[22\left(\frac{\sigma_{ff}}{r}\right)^{12} - 5\left(\frac{\sigma_{ff}}{r}\right)^{6}\right]. \quad (6)$$

Based on the analysis of Sese [30], the effective potential given by Eq. (2) is reliable for a particle with the reduced de Broglie thermal wavelength λ_B^*<0.5, where

$$\lambda_B^* = h/\left(2\pi m k_B T\sigma_{ff}^2\right)^{1/2} \quad (7)$$

The λ_B^* value for hydrogen at 77 K is 0.47.

To be able to compare our calculations with published results, we start with the slit pore model that is one-dimensional with respect to the z-axis perpendicular to the ideal uniform surface of a graphitic solid. The potential of interactions $\phi_{sf}(z)$ of a gas molecule with such a model solid depends only on a distance from the center of the molecule to the centers of carbon atoms in the solid surface and is expressed as a sum of interaction potentials with the single surface layer of graphite ϕ_l and interactions and interactions with the rest of the solid. This potential is usually given by the Steele formula [31]

$$\phi_{sf}(z) = \phi_1(z) + \phi_\infty(z), \quad (8)$$

where ϕ_l is evaluated by the integration of the LJ potential over the surface,

$$\phi_1(z) = A\left[\frac{2}{5}\left(\frac{\sigma_{sf}}{z}\right)^{10} - \left(\frac{\sigma_{sf}}{z}\right)^{4}\right], \quad (9)$$

and ϕ_∞ is represents the interaction potential with other graphite layers summed up to infinity

$$\phi_\infty(z) = -\frac{A\sigma_{sf}^4}{3\Delta(z+0.61\Delta)^3} \quad (10)$$

The aggregate parameter A is given by

$$\mathrm{A} = 2\pi{\sigma_{sf}}^2\varepsilon_{sf}\rho_s\Delta \quad (11)$$

where ε_{sf} and σ_{sf} are the solid-fluid energy and size interaction parameters, ρ_s is the density of carbon atoms in graphite, and Δ is the spacing between graphite layers.

The FH correction for the interaction potential of H_2 molecule with a single graphitic plane is obtained by applying formula (3) to the solid-fluid LJ potential and integrating over the plane surface which gives the following expression:

$$\phi^q_{sheet}(z) = QAz^{-2}\left[\frac{11}{6}\left(\frac{\sigma_{sf}}{z}\right)^{10} - \frac{5}{6}\left(\frac{\sigma_{sf}}{z}\right)^{4}\right] \quad (12)$$

The Steele potential [31] given by Eq. (8) sums interactions with the series of parallel graphitic planes expanded to ∞. The FH correction for the graphitic pore wall is given here by the following finite sum:

$$\phi^q_{sf}(z) = \sum_{i=0}^{4}\phi^q_{sheet}(z + i\Delta) \quad (13)$$

A similar formula was derived earlier [32], and it is justified by the fact that terms in this sum decrease sharply with the distance from the surface.

The total quantum-corrected external potential of interaction between H_2 molecule and standard slit pore may now be written as

$$V^{FH}_{st.slit}(z) = \phi_{sf}\left(\frac{H}{2} + z\right) + \phi_{sf}\left(\frac{H}{2} - z\right) + \phi^q_{sf}\left(\frac{H}{2} + z\right) + \phi^q_{sf}\left(\frac{H}{2} - z\right), \quad (14)$$

Where pore width H is the distance between the centers of atoms composing the surface planes of the opposite walls.

For the comparison of our quantum corrected NLDFT calculations with published results, we used Eq. (14) as the external potential in Eq. (1) and we calculated several FH-NLDFT adsorption isotherms of H_2 at 77 K using ε_{ff}/k_B = 36.7 K and σ_{ff} = 2.958 Å as the LJ fluid-fluid interaction parameters [33]. The solid–fluid parameters were obtained from the Lorentz-Berthelot combining rules taking the values ε_s/k_B =28 K and σ_s = 3.4 Å for the carbon-carbon interaction parameters in graphite [31]. The same LJ parametrization was applied for the modeling of H_2 isotherms at 77 K in three reference papers: (a) [32], (b) [12] and (c) [34]. The method used in (a) and (b) papers was the grand canonical Monte Carlo (GCMC) simulation with FH quantum correction FH-GCMC while the method used in the paper (c) was the path-integral PI-GCMC method, which is considered the most accurate treatment of the thermodynamics of quantum fluids. We digitized the data of Fig. 2, Fig. 6a, and Fig. 2a from papers (a), (b), and (c), respectively. The isotherms data were converted to common format and compared with the FH-NLDFT isotherms in Fig. 1. The H_2 isotherms are expressed as the mass

densities calculated per volume between pore walls separated by the distance *H*. The plotted isotherms are labeled with values of the effective pore width [35] defined as $w = H - 3.4$ Å.

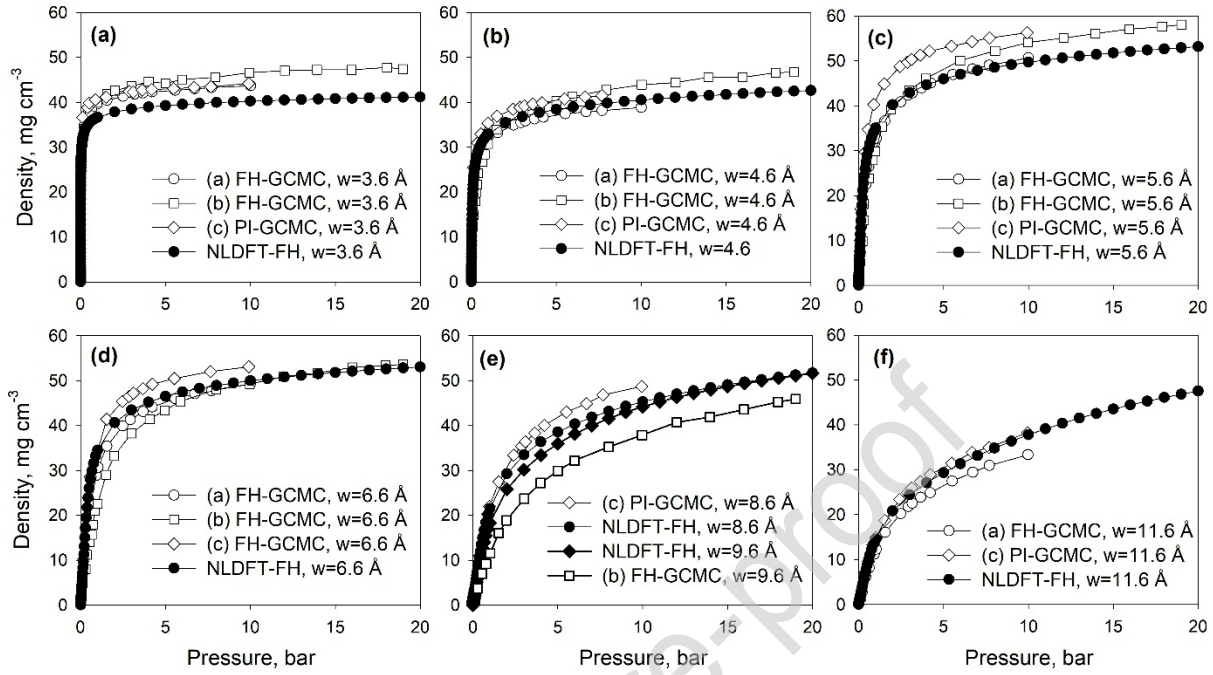

Fig. 1- Comparison of quantum corrected absolute NLDFT-FH isotherms calculated in the present work with literature data calculated using (quantum corrected) FH-GCMC and (path integral) PI-GCMC. Data taken from three reference papers: (a) [32], (b) [12] and (c) [34].

The theoretical isotherms (Fig. 1) calculated using three different methods are highly similar, but not identical. The sequence of the isotherm values is not the same for different pore sizes. The NLDFT-FH isotherms calculated in the present work show values in between the values of other isotherms or slightly below other values in only one case of pore width *w*=3.6 Å (Fig. 1a). Taking into account the complexity of the methods used in the calculations of the data presented in Fig. 1 and their certain diversity, we may consider our NLDFT-FH results in an overall agreement with the other referenced data.

3.1.2 Two-dimensional slit pore model with quantum corrections

The two-dimensional model used in the present work assumes the corrugated and energetically heterogeneous surface of carbon pores [21, 22]. The model was formulated on the bases of the graphene carbon structure that was demonstrated in the recent study [36] using atomic-resolution images obtained from STEM microscopy. The images presented in that study were taken from various parts of nanoporous carbon samples, and they consistently showed the curved and defective graphene sheets that, according to the authors, constitute the carbon

building blocks. To describe the spatial curvature of the surface, it is necessary to extend the description of the solid-fluid interaction potential from one-dimensional $\phi_{sf}(z)$, used in the standard model, to at least two-dimensional $\phi_{sf}(x, z)$. In the present model, ϕ_{sf} is constant as a function of y variable, and a simple trigonometric function describes the corrugation of the graphene pore surfaces,

$$t(x) = \alpha \sin(2\pi x/\lambda), \tag{15}$$

where α is the amplitude and λ is the periodicity of the corrugation.

In addition to the corrugation, the surface is energetically heterogeneous, where a trigonometric series describes this heterogeneity

$$E(x) = 1 + \sum_{k=1}^{n} \beta_k \sin(2\pi k x/\lambda), \tag{16}$$

where n is the number of β_k adjustable parameters.

The corrugation and the energetic heterogeneity are introduced only to the carbon surface layer. The solid-fluid potential $\phi_l(x, z)$ for this layer and its FH quantum correction ϕ_1^q are calculated by the integration of the LJ potential and its quantum correction. First, an analytical integration over the y-direction gives the following integrals of one variable:

$$\phi_1(x,z) = A\int_{-\infty}^{\infty} \frac{E(x')}{q}\left[\frac{63}{512}\left(\frac{\sigma_{sf}}{q}\right)^{10} - \frac{3}{16}\left(\frac{\sigma_{sf}}{q}\right)^{4}\right] g\, dx' \tag{17}$$

$$\phi_1^q(x,z) = QA\int_{-\infty}^{\infty} \frac{E(x')}{q^3}\left[\frac{3531}{1024}\left(\frac{\sigma_{sf}}{q}\right)^{10} - \frac{25}{32}\left(\frac{\sigma_{sf}}{q}\right)^{4}\right] g\, dx' \tag{18}$$

where

$$g = \left[1 + (dt/dx')^2\right]^{1/2} \tag{19}$$

$$q = \left[(z + t(x'))^2 + (x - x')^2\right]^{1/2} \tag{20}$$

Then, the numerical integration using the ten point Gaussian quadrature is performed to evaluate the integrals in Eqs. (17) and (18). To calculate these integrals in infinite limits the periodic boundary conditions are assumed for the x coordinate.

Finally, using Eqs. (10) (12) (17) (18) the corrugated wall potential with quantum-corrections may be expressed in the following form:

$$V_{wall}^{FH}(x,z) = \phi_1(x,z) + \phi_\infty(z + \alpha) + \phi_1^q(x,z) + \sum_{i=1}^{4} \phi_{sheet}^q(z + \alpha + i\Delta), \tag{21}$$

where the amplitude α is added to shift potentials ϕ_∞ and ϕ^q_{sheet} from ϕ_1 to avoid geometrical overlapping with the corrugated surface layer.

The potential defined by Eq. 21 is used in Eq. (1) as the external potential to calculate the theoretical adsorption isotherm (2D-HS-FH) on the model carbon surface. This isotherm is fitted to the experimental H_2 isotherm on the reference carbon black BP 280 (Fig. 2) to obtain the energetic heterogeneity parameters and the ε_{sf} parameter of our H_2 adsorption model. This reference carbon has been consistently used to develop the 2D-HS models for other gases [2, 16, 22]. The other interaction parameters are the same as for standard slit pore model (section 3.1.1). The surface corrugation is assumed here to be the same as established for the original 2D-HS nitrogen model [22], but since the surface geometrical parameters, α and λ are expressed in terms of the reduced quantities scaled with respect to the molecular diameter; we adjusted these parameters accordingly for H_2 molecule to preserve the corrugation geometry. All parameters applied in the 2D-HS-FH model calculations are reported in Table 1. For comparison, Table 1 also contains the parameters used in the original 2D-HS model for N_2 [22, 37].

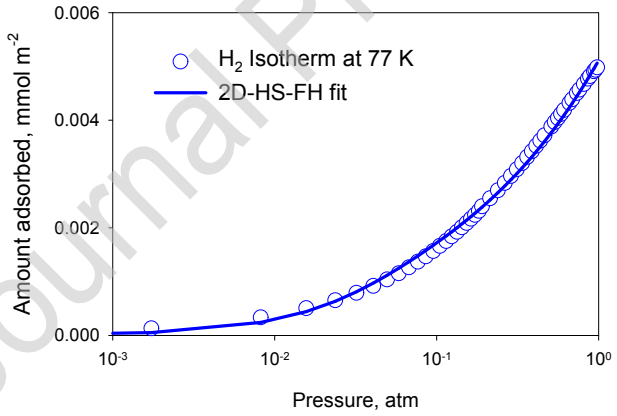

Fig. 2- Fit of the 2D-HS-FH model to the experimental isotherm of H_2 measured at 77 K on the reference carbon black BP 280.

Table 1. Parameters used to calculate the 2D-HS-FH kernel for H_2 and 2D-HS kernel for N_2 adsorption at 77 K on carbons with heterogeneous surfaces.

Intermolecular interaction parameters	H_2	N_2	Heterogeneity parameters	H_2	N_2
$\sigma_{ff}=d_{HS}$(Å)	2.96	3.58	β_1	0.357	0.065
ε_{ff}/k (K)	36.70	93.62	β_2	0.640	0.565
σ_{sf} (Å)	3.18	3.49	α	0.54	0.45
ε_{sf}/k (K)	32.86	53.50	λ	7.0	6.0

The total quantum corrected external potential of H_2 interaction with the corrugated pore is given as sum of the wall potentials defined by Eq. (21),

$$V_{pore}^{FH}(x,z) = V_{wall}^{FH}\left(x,\frac{H}{2}+z\right) + V_{wall}^{FH}\left(x,\frac{H}{2}-z\right) \qquad (22)$$

A detailed description of a corrugated pore model and the calculation method of the theoretical isotherms have been given earlier [2, 22]. Here, we calculated the kernel of 2D-HS-FH theoretical isotherms for H_2 at 77 K using the parameters listed in Table 1. This kernel constitutes our quantum-corrected hydrogen model for carbons with the heterogeneous surface. Fig. 3a shows the excess isotherms of this model for selected effective pore widths, w. To illustrate the effect of FH quantum corrections, the isotherms calculated without these corrections are also shown in this figure. The fact that the quantum corrected model predicts lower H_2 densities than the classical model is because the quantum effects weaken the fluid-fluid and solid-fluid interactions [12, 38]. To compare the H_2 kernel with the previously developed CO_2 kernel [16], in Fig. 3b, we plot the 2D-HS isotherms of CO_2 at 273 K calculated for the same pore widths as for H_2. The absolute pressures of 1 and 10 atm correspond to 0.03 and 0.3 p/p_0 for CO_2. It is interesting to note that both sets of isotherms are similar in shape, but CO_2 isotherms show lower densities and are shifted to higher pressures compared to H_2 isotherms. These differences between the two kernels indicate that the H_2 kernel is to a certain extent more responsive to pore sizes than CO_2 kernel under the temperature and experimental pressure conditions.

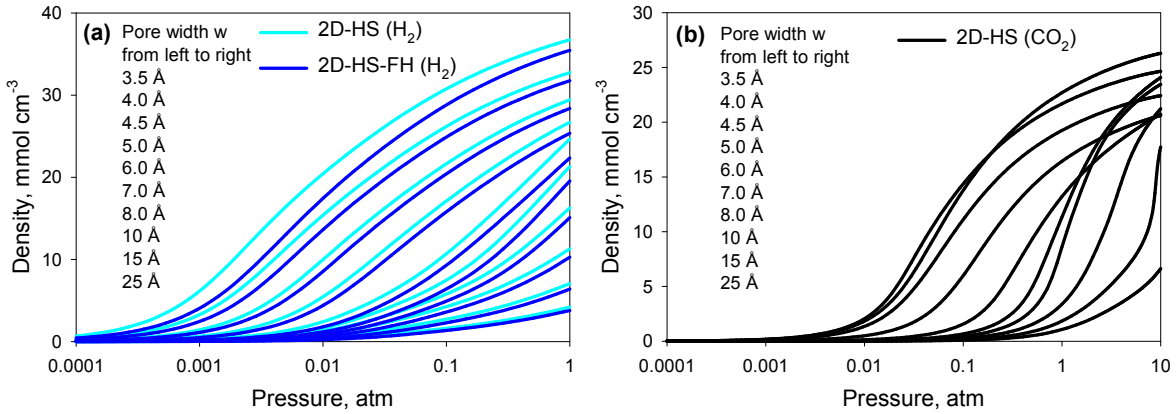

Fig. 3- The excess theoretical adsorption isotherms of 2D-HS kernels for H_2 at 77 K (a) and CO_2 at 273 K (b) calculated for selected effective pore widths, w from 3.5 to 25 Å.

It is important to realize that both kernels presented in Fig. 3 have limited applicability for the PSD characterization of porous carbons. As discussed earlier [16, 39], the sensitivity of CO_2 adsorption isotherms to pore sizes is limited to $w \approx 10$ Å. A similar upper sensitivity limit was considered [40] for H_2 at 77 K. At this temperature, H_2 is a supercritical gas which does not condense. Its adsorption isotherms are of type I (Fig. 3a), and their shapes for larger pores become increasingly more similar to one another, which in mathematical terms means that they become linearly dependent, and thus less sensitive to pore sizes. To better explain the physical state of H_2 gas confined in the carbon micropores, we plot in Fig 4, the density profiles in the pores of different widths calculated by the present 2D-HS model. This illustration shows that at 77 K and 1 atm H_2 may saturate only the small pores of 4 – 7 Å. The average density of H_2 decreases in larger pores where it is adsorbed mostly on the pore walls. It follows that the amount of H_2 adsorbed in the larger pores depends on their surface area and not on their widths.

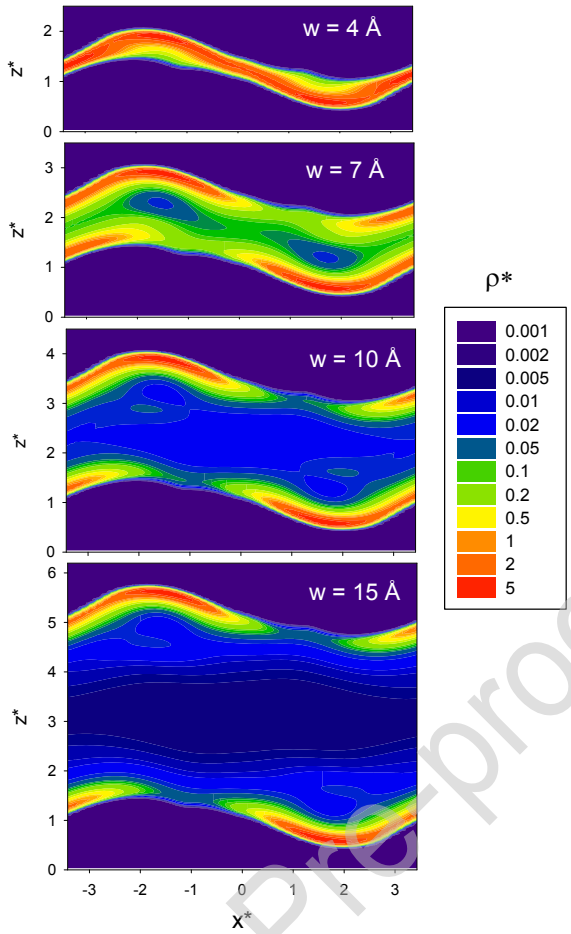

Fig. 4- Cross-sectional contours of the local densities of H_2 at 77 K and 1 atm calculated using present 2D-HS-FH model.

The limited sensitivity to larger pore sizes of CO_2 and H_2 implies that to calculate the carbon PSD in a full range of micro and mesopores, it is necessary to use an additional adsorbate that will condense in the larger pores. The concept of using two adsorbates that are sensitive to different pore sizes was implemented for CO_2 and N_2 in the dual gas analysis method [16, 24]. A similar methodology has been applied earlier using standard NLDFT [11, 40] and GCMC [12, 41] models.

3.2 Comparison of the PSD characterization methods using multiple simple gases

It was recently demonstrated that the PSD results obtained from the 2D-HS models and adsorption isotherms of N_2, Ar, and O_2 [2] were consistent for several representative porous carbons. Here, we attempt to show that the dual gas analysis methods based on two pairs of simple gases, N_2 and CO_2, and O_2 and H_2 also give consistent results in terms of carbon PSDs. We use the adsorption data of N_2, and CO_2 reported in two papers [16, 24] for two series of

porous carbons and new adsorption data of O_2 and H_2 measured at 77 K on the same carbons. All PSD were calculated using the SAIEUS [42] software that is available at www.nldft.com.

The results of the PSD analysis of PC series of samples are presented in Figs. 5 and 6. The PC samples are the activated carbons with systematically changing pore structures upon the increasing degree of activation. The sample labeled PC is a char derived from PET, and the activated carbons derived from this char by CO_2 activation are labeled PCn, where n is the burn-off percent. The goodness of fit of the 2D-HS models to the isotherms measured on these samples is shown in Fig. 5 where we plot experimental data and fitting lines in a linear and logarithmic pressure scale to show the goodness of fit accurately in the range of low and high pressures. Meanwhile, it is interesting to note that the amounts adsorbed of H_2 measured up to 1 atm reach values similar to those of CO_2 measured up to 10 atm. The CO_2 uptake on these carbons at 1 atm is significantly smaller than H_2 at the same pressure.

The isotherms of carbons with narrow PSDs (PC, PC5, and PC23) were fitted using dual gas analysis method applied to two pairs of isotherms, N_2 & CO_2, and O_2 & H_2. The version of the dual gas analysis method introduced in the original reference [16] was unable to fit the 2D-HS models simultaneously to N_2 & CO_2 isotherms for samples of char PC (Fig. 5 a1, b1) and mildly activated char PC5 (Fig. 5 a2, b2) . These samples have extremely small ultramicropores which hinder the diffusion of N_2 at low temperature and pressure. The problem was then solved by fitting partial data excluding the N_2 data points at pressures below 0.001 p/p_0 and the CO_2 points above 0.03 p/p_0.

Here, we apply a refined approach to this problem [24], and we slightly increase the lower pore width limit w_{min} of the N_2 kernel. With this modification, we are able to fit simultaneously both isotherms in the full range of pressures. The physical meaning of w_{min} is an estimate of the minimum pore width accessible to N_2 molecules at the measurement conditions. Increasing the w_{min} parameter from its default value w_{min} = 3.6 Å modifies the N_2 kernel by excluding the theoretical isotherms calculated for small pores that contribute to CO_2 but not to N_2 adsorption at low temperature and pressure. We believe that this approach is more accurate and provides higher resolution than the approach that excludes the experimental points as it was done previously.

The comparison of PSDs obtained from the two pairs of gases N_2 & CO_2, and O_2 & H_2 show similarities and differences. As reported in Table 1, the H_2 molecule has a smaller molecular diameter ($\sigma_{ff} \cong 3$ Å) than the other gases used in this work which means it may access smaller pores than the other gases. Consequently, we assumed w_{min} = 3.0 Å for the H_2 kernel, and thus we extended the range of the PSD analysis using this gas to the lower limit than can be achieved

by other gases. As a result, the PSDs of PC, PC5, and PC23 (Fig. 5 a1-a3) calculated using O_2 & H_2 have similar shapes to those derived from N_2 & CO_2 but are shifted to lower pore sizes showing an additional contribution to pore volume by the smallest pores accessible to H_2 but not to other gases. These additional pore volumes are visible in the cumulative pore volume plots (Fig. 5 b1-b3) and are reported in Table 2.

For carbons with wider PSDs (PC39 and PC63), we were able to obtain excellent fit of four 2D-HS models to four isotherms simultaneously which implies that the PSDs calculated for these carbons from the general fit of four isotherms should be very similar to those obtained from two gases N_2 & CO_2 being a subset of the four gases. Indeed, this similarity is confirmed by the calculated PSDs and pore volumes (Fig. 6 and Table 2). Results of simultaneous fitting of the NLDFT kernels to adsorption data of several gases measured on the same sample were reported earlier [16, 40, 43]. The results derived from such a procedure are statistically more robust than those derived from a single isotherm. Moreover, if the goodness of such fit is satisfactory, it confirms that the obtained PSDs are not adsorbate related.

Table 2. Cumulative pore volumes calculated from the kernel sets including H_2 model. Comparison with volumes calculated from the dual gas N_2 & CO_2 using 2D-HS models.

Sample	Pore volume from the kernel set including H_2 model [cm^3g^{-1}] *Pore volume difference from N_2 & CO_2 model [%]*				
	w <6 Å	w <10 Å	w <15 Å	w <20 Å	w <50 Å
PC	0.14 *43%*	0.24 *24%*	0.25 *23%*	0.26 *24%*	0.26 *24%*
PC5	0.16 *23%*	0.22 *2%*	0.26 *13%*	0.26 *14%*	0.28 *17%*
PC23	0.18 *34%*	0.31 *9%*	0.39 *3%*	0.43 *3%*	0.43 *0%*
PC39	0.15 *7%*	0.38 *6%*	0.54 *5%*	0.63 *4%*	0.65 *3%*
PC63	0.08 *-2%*	0.33 *1%*	0.57 *2%*	0.84 *2%*	1.07 *-1%*
C-CS	0.09 *1%*	0.12 *13%*	0.13 *18%*	0.14 *22%*	0.14 *22%*
C-CS-0.5	0.16 *33%*	0.22 *10%*	0.25 *11%*	0.25 *9%*	0.29 *6%*
C-CS-1.0	0.16 *21%*	0.25 *1%*	0.31 *4%*	0.33 *4%*	0.37 *2%*

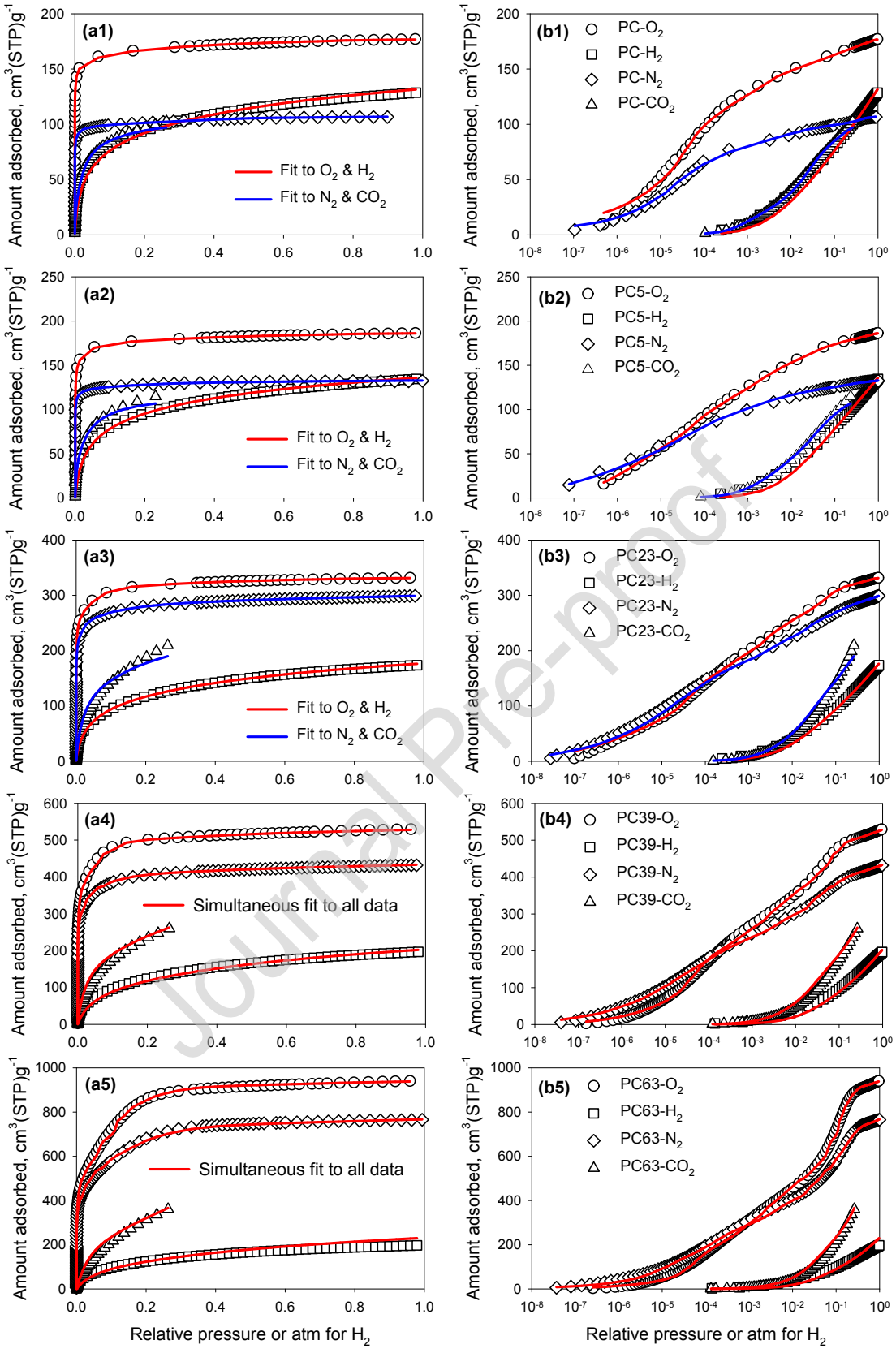

Fig. 5 –Multiple gas analysis of the PC series of samples on the basis of the 2D-HS models. Simultaneous fits of the models to two or four isotherms of O_2, H_2, and N_2 at 77 K, and CO_2 at 273 K plotted in linear (a) and logarithmic (b) pressure scale.

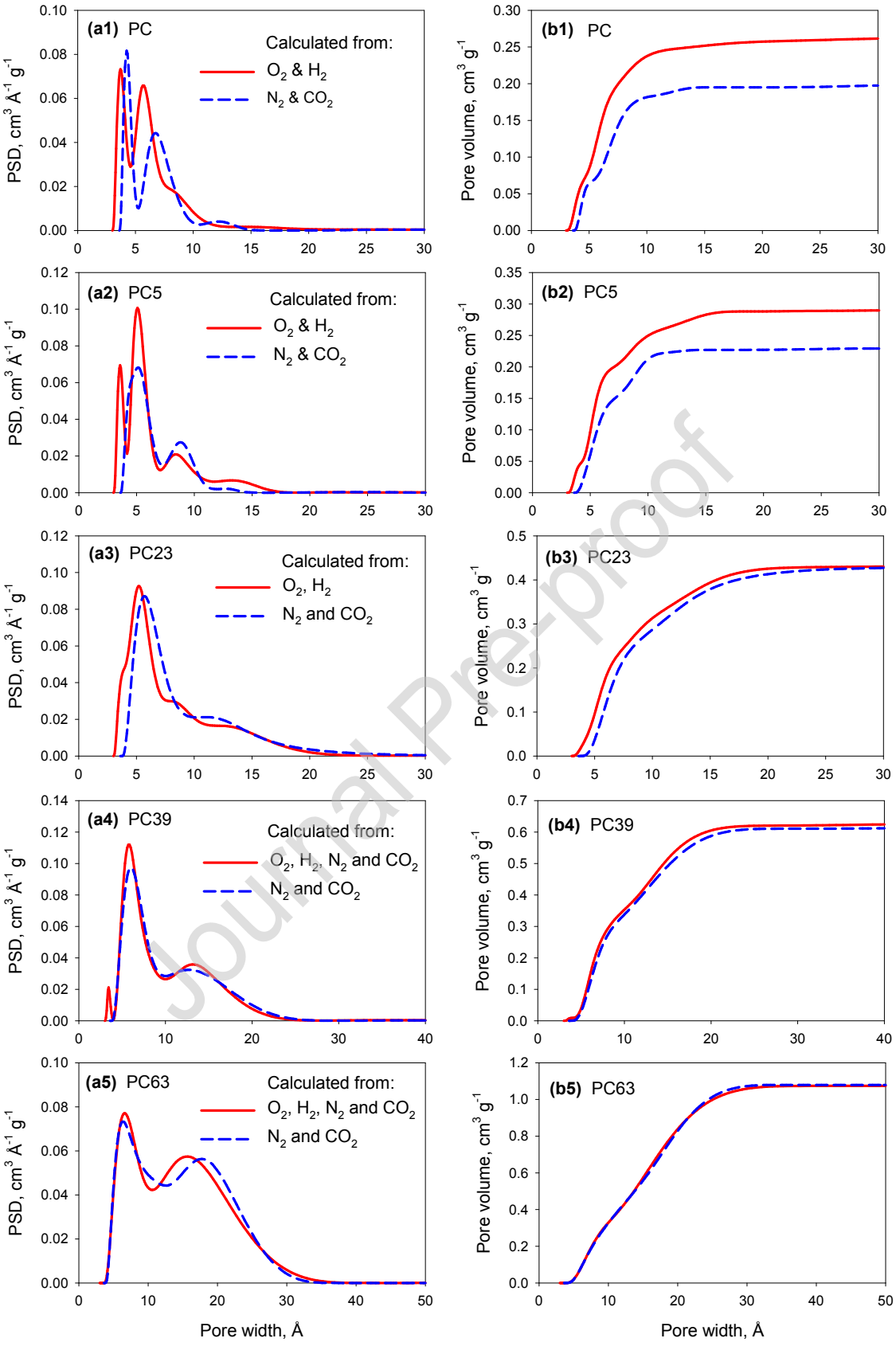

Fig. 6 – Results of the multiple gas analysis of the PC series of samples on the basis of the 2D-HS models. Comparison of the differential PSDs (a) and cumulative pore volumes (b) derived from the dual fit of N_2 & CO_2 pair of isotherms versus O_2 & H_2 or all four isotherms.

The samples of the second series of carbons C-CS are all characterized by the narrow PSDs. Nevertheless, we were able to fit simultaneously four 2D-HS models to four respective isotherms for two carbon samples C-CS-0.5 (Figs. 7 a2 & b2) and C-CS-1.0. (Figs. 7 a3 & b3). Only C-CS sample that is a non-activated char requires separate fitting of the two pairs of isotherms with two dual models N_2 & CO_2, and O_2 & H_2. In general, a high similarity is observed between the PSDs derived from the two types of analysis for the C-CS carbon series.

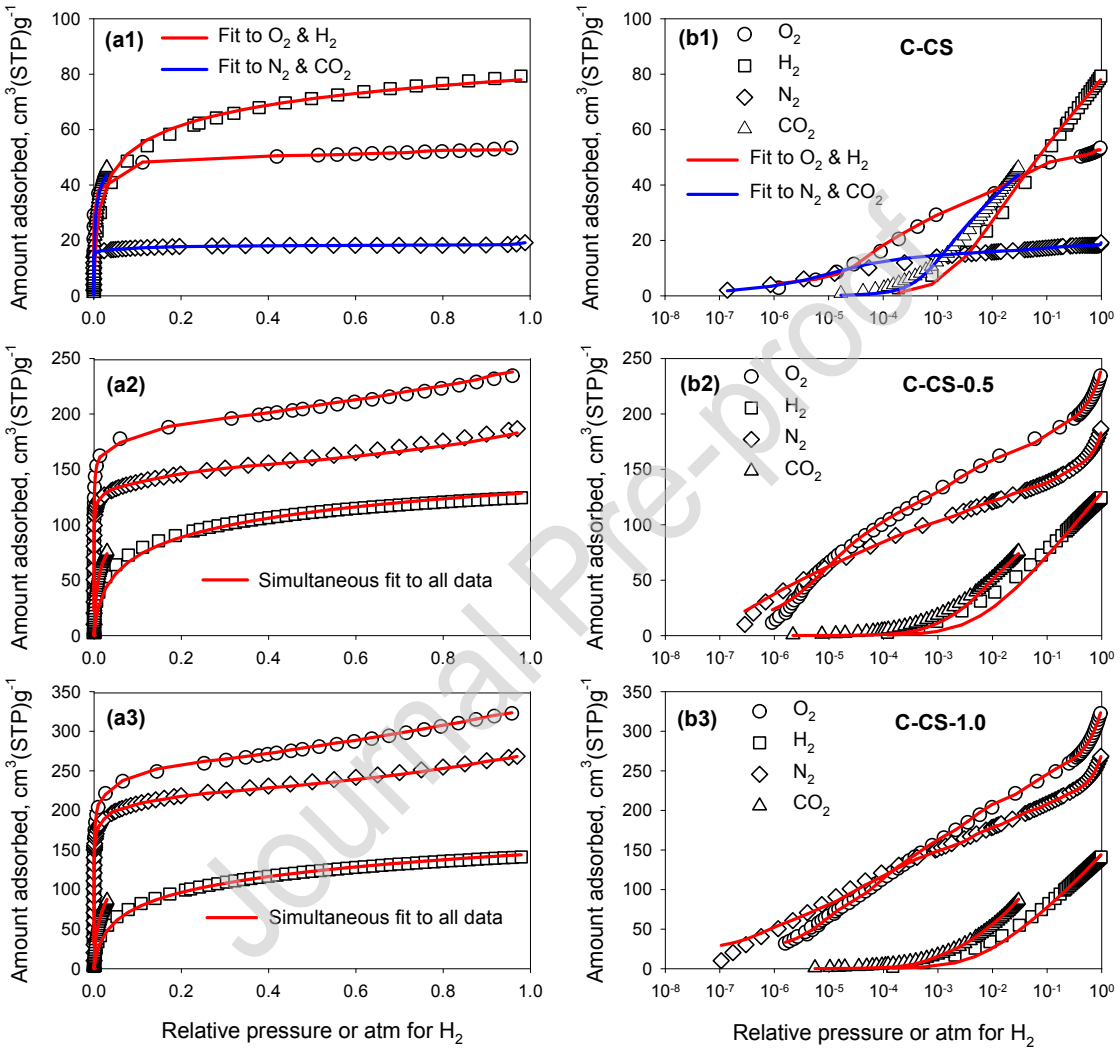

Fig. 7 – Multiple gas analysis of the CS series of samples on the basis of the 2D-HS models. Notation is the same as in Fig. 5.

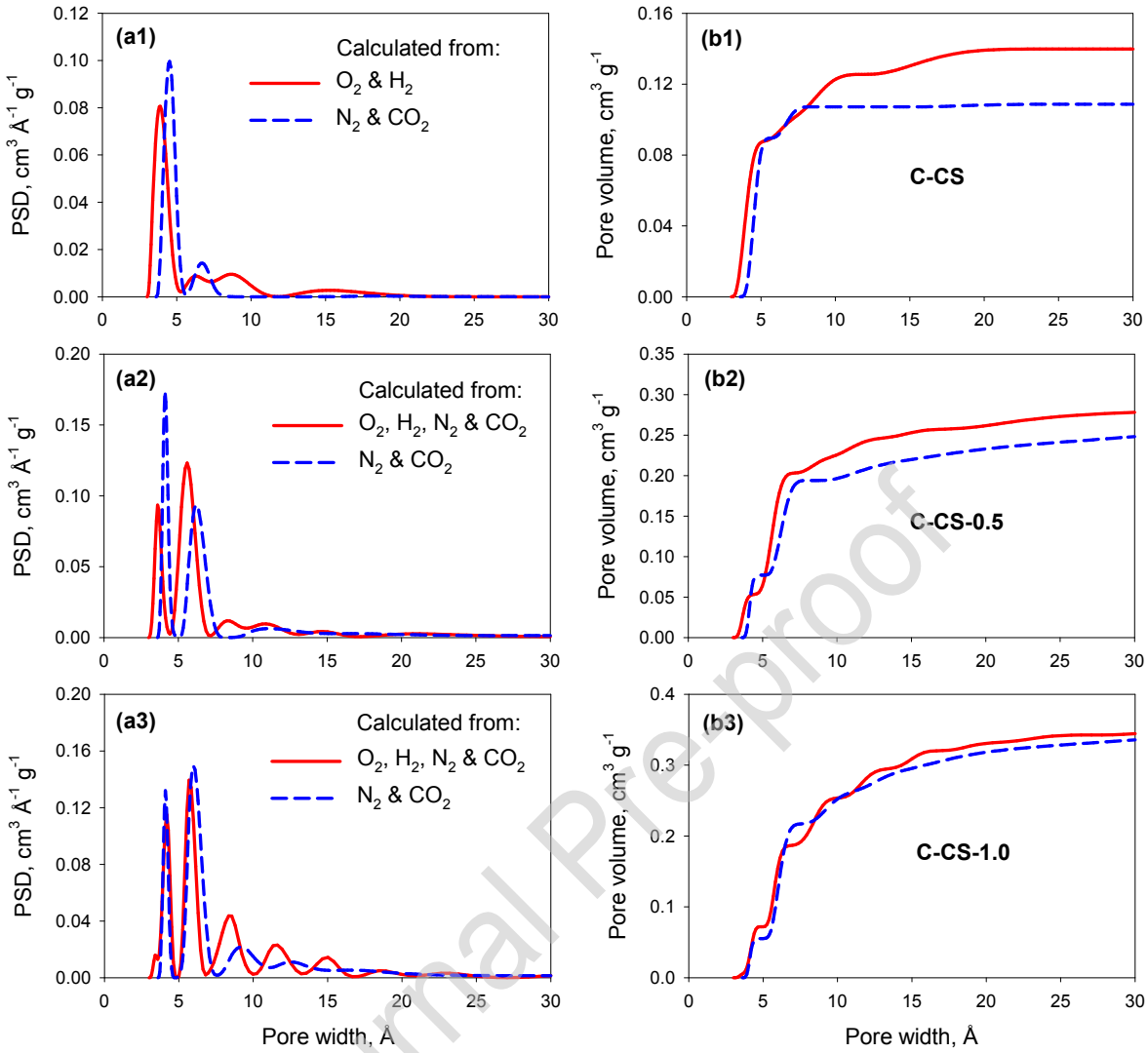

Fig. 8 - Results of the multiple gas analysis of the CS series of samples on the basis of the 2D-HS models. Notation is the same as in Fig. 6.

3.3 Dual gas analysis using full H_2 isotherm and O_2 isotherm without-low pressure data

The comparisons presented in the preceding section show consistency between the results derived from the pairs of isotherms N_2 & CO_2, and O_2 & H_2 and in some cases between all four gases. This consistency is demonstrated by the ability of simultaneous fit of two or four 2D-HS models to the relevant isotherms. The fitted isotherms are, in part, mathematically correlated via applied models and the calculated PSD. This correlation is limited to the range of pore sizes to which both models are sensitive. The original work on the dual gas analysis method [16] took advantage of this correlation and showed, using PC23 and PC85 samples as examples, that the analysis of N_2 isotherm at 77 K without low-pressure data in combination with CO_2 isotherm

at 273 K might give the PSD equivalent to that derived from the full N_2 isotherm. Here, we follow that approach and apply it to O_2 & H_2 data of two samples, PC23 (Fig. 9) and C-CS (Fig. 10). In both cases, the PSDs derived from full data of both isotherms are in a close agreement with the PSDs derived from full H_2 and partial O_2 isotherms. By partial O_2 isotherm, we mean the isotherm without low-pressure points shown as full symbols in Figs. 9 and 10.

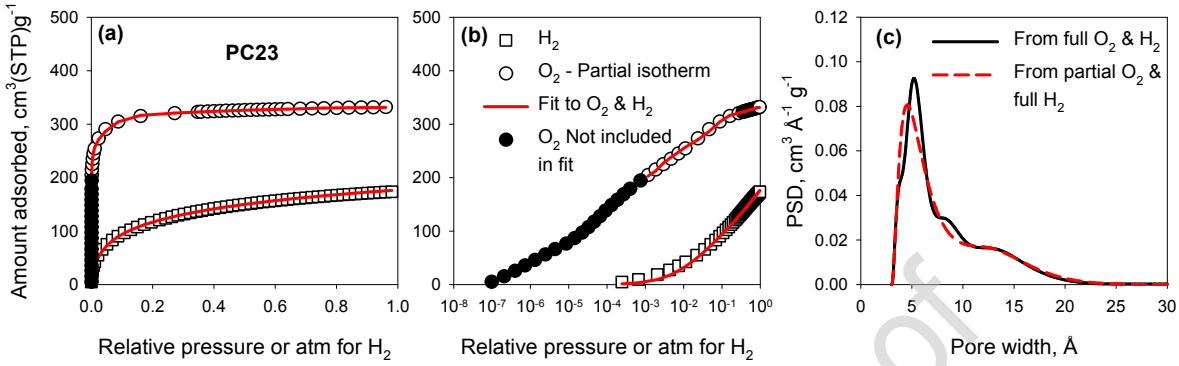

Fig. 9 – PSD analysis of PC23 sample. Simultaneous fit of 2D-HS models to full H_2 isotherm and partial O_2 isotherm in linear (a) and logarithmic (b) scale. (c) Comparison of the differential PSDs derived from H_2 and partial O_2 isotherms with the PSDs derived from full data of both isotherms.

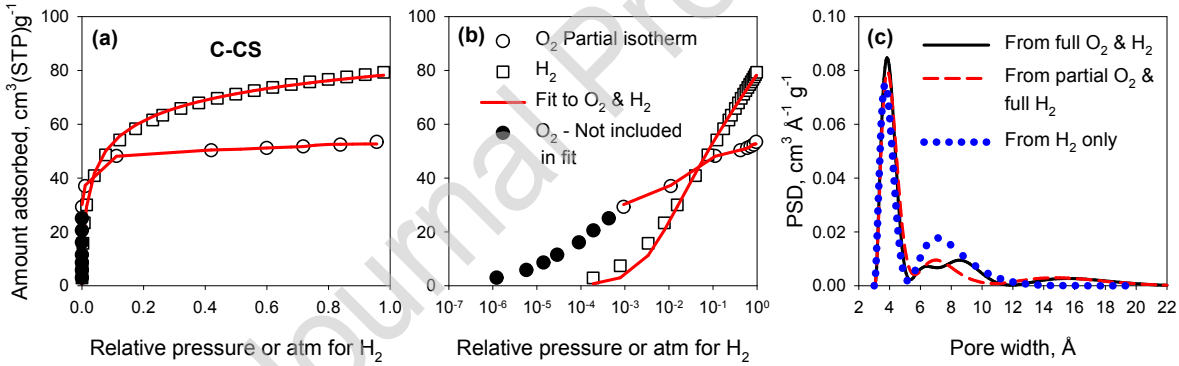

Fig. 10 – PSD analysis of C-CS sample. Notation is the same as in Fig. 9.

To explain the validity of the presented approach in simple terms, we note that the full O_2 isotherm may provide the information about the full range of micro and mesopores, while the information limited to small pores is provided by H_2 isotherm. It follows that in combination with H_2 isotherm only upper-pressure part of O_2 isotherm is necessary to describe the full range of micro and mesopores. At this point, it is interesting to note that in special cases of ultramicroporous carbons, a single H_2 isotherm may be sufficient for evaluating the carbon PSD. Such a result is presented as a dotted line in Fig. 10c for ultramicroporous char C-CS. This result could be expected based on the fact that the H_2 uptake for this carbon is higher than O_2.

Finally, following the suggestion of one of the reviewers, we consider N_2 & H_2 as another combination of gases to be employed in the dual gas method. Some researchers may find it convenient to continue using standard N_2 adsorption for carbon materials that are not expected to have a significant amount of the surface polar sites, combine N_2 & H_2 data measured at 77 K for the analysis with the dual gas method. To show that such an approach may be effective, in Fig. 11, we present the results of the dual gas analysis using N_2 & H_2 for the sample of PC char. As in the case of O_2 & H_2 analysis shown in Fig. 9 and 10, we observe a high similarity between the PSDs derived using N_2 isotherm data in the full and reduced pressure scale. This example demonstrates the general applicability of the dual gas analysis method that may employ various gases chosen based on their molecular properties, such as the molecular diameter or the intermolecular interaction parameters.

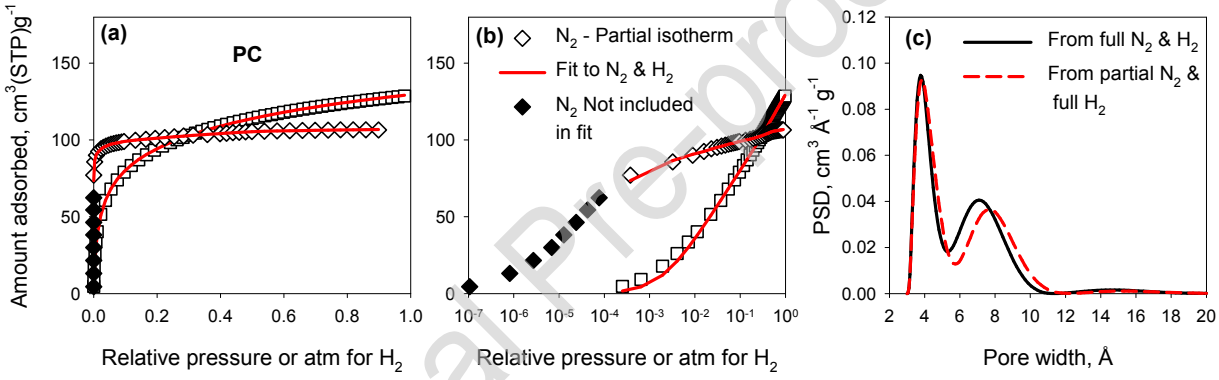

Fig. 11 – PSD analysis of PC sample. Notation is the same as in Fig. 9, but for N_2 instead O_2.

4. Conclusions

This study is an extension of previous studies [16, 24] on the dual gas analysis method using N_2 and CO_2 isotherms, which we propose to replace with the analysis of O_2 & H_2 isotherms. In the first part of this work we develop the quantum corrected 2D-HS-FH model for H_2 adsorption on the heterogeneous carbon surface at 77 K. This model is then used in conjunction with the earlier developed O_2 model for the carbon PSD analysis at 77 K.

The underlying reason of using the isotherms of fast diffusing gases like CO_2 at 273 K or H_2 at 77 K in combination with the N_2 or O_2 isotherms is to obtain reliable information about carbon micro and ultramicropore sizes. The diffusion of CO_2 into micropores at 273 K is faster than N_2 at 77 K, which makes the measurement of equilibrium adsorption data more reliable and obtained faster. The same refers to H_2 adsorption as H_2 is a supercritical gas at 77 K.

The drawback of using N_2 and CO_2 is their high quadrupole moment that may influence the measured isotherms by interacting with the surface polar sites. A replacement of these gases with O_2 and H_2 that have significantly smaller quadrupole moments than the other pair of gases. To quantify the effects of such substitution, we compare the PSD analysis results using the pairs of isotherms N_2 & CO_2, and O_2 & H_2 for several reference carbon samples and the comparisons show consistency between the results derived from both pairs of isotherms. For samples with wider PSDs, we were able to fit the relevant 2D-HS models to adsorption data of all four gases simultaneously and as a result, obtain a common PSD from all data.

Samples with narrow PSDs require separate fitting using two dual models N_2 & CO_2, and O_2 & H_2. Because H_2 molecule has a smaller molecular diameter (σ_{ff} = 3 Å) than the other gases it can penetrate smaller pores and the range of PSD analysis using this gas may be extended to a lower limit than the standard for N_2 by about 0.5 Å. As a result, the PSDs calculated using O_2 & H_2 have similar shapes to those derived from N_2 & CO_2 but are shifted to lower pore sizes showing an additional contribution to pore volume by the smallest pores accessible to H_2 but not to other gases. These additional pore volumes are visible in the cumulative pore volume plots.

A fundamental and practical benefit of using the dual gas analysis method is the ability of obtaining the full micro and mesopore PSD by using a partial O_2 isotherm without low-pressure data in combination with full H_2 isotherm both measured at 77 K. We presented examples for our reference samples where the PSDs derived from full data of both isotherms are in a close agreement with the PSDs derived from full H_2 and partial O_2 isotherms. By partial O_2 isotherm, we mean the isotherm without low-pressure points, $p/p_0<10^{-3}$.

We also showed that in special cases of ultramicroporous carbons where the H_2 uptake is higher than O_2, a single H_2 isotherm might be sufficient for evaluating the carbon PSD. Using this option may be very useful for screening the properties of such materials as chars, biochars, and carbon molecular sieves.

We believe that the results and methods presented in this study may facilitate obtaining highly detailed characteristics of microporous carbon materials. Such detailed and accurate characteristics are critical for the advanced carbon applications such as electrodes in supercapacitors [44], gas storage [6], gas sensors [45, 46], or gas separation using molecular sieves [47].

References

[1] M. Thommes, K. Kaneko, A.V. Neimark, J.P. Olivier, F. Rodriguez-Reinoso, J. Rouquerol, K.S. Sing, Physisorption of gases, with special reference to the evaluation of surface area and pore size distribution (IUPAC Technical Report), Pure and Applied Chemistry 87 (2015) 1051-1069.
[2] J. Jagiello, J. Kenvin, Consistency of carbon nanopore characteristics derived from adsorption of simple gases and 2D-NLDFT models. Advantages of using adsorption isotherms of oxygen (O2) at 77 K, Journal of Colloid and Interface Science 542 (2019) 151-158.
[3] M. Seredych, J. Jagiello, T.J. Bandosz, Complexity of CO2 adsorption on nanoporous sulfur-doped carbons – Is surface chemistry an important factor?, Carbon 74 (2014) 207-217.
[4] J. Garrido, A. Linares-Solano, J.M. Martin-Martinez, M. Molina-Sabio, F. Rodriguez-Reinoso, R. Torregrosa, Use of nitrogen vs. carbon dioxide in the characterization of activated carbons, Langmuir : the ACS journal of surfaces and colloids 3 (1987) 76-81.
[5] D. Lozano-Castelló, D. Cazorla-Amorós, A. Linares-Solano, Usefulness of CO2 adsorption at 273 K for the characterization of porous carbons, Carbon 42 (2004) 1233-1242.
[6] S. Schaefer, V. Fierro, M.T. Izquierdo, A. Celzard, Assessment of hydrogen storage in activated carbons produced from hydrothermally treated organic materials, International Journal of Hydrogen Energy 41 (2016) 12146-12156.
[7] S. Schaefer, V. Fierro, A. Szczurek, M.T. Izquierdo, A. Celzard, Physisorption, chemisorption and spill-over contributions to hydrogen storage, International Journal of Hydrogen Energy 41 (2016) 17442-17452.
[8] H. McLaughlin, F. Shields, J. Jagiello, G. Thiele, Analytical options for biochar adsorption and surface area, North American Biochar Conference, Sonoma, CA, 2012.
[9] J.N. Caguiat, D.W. Kirk, C.Q. Jia, Uncertainties in characterization of nanoporous carbons using density functional theory-based gas physisorption, Carbon 72 (2014) 47-56.
[10] A.D. Lueking, H.-Y. Kim, J. Jagiello, K. Bancroft, J.K. Johnson, M.W. Cole, Tests of Pore-Size Distributions Deduced from Inversion of Simulated and Real Adsorption Data, Journal of Low Temperature Physics 157 (2009) 410-428.
[11] J. Jagiello, W. Betz, Characterization of pore structure of carbon molecular sieves using DFT analysis of Ar and H2 adsorption data, Microporous and Mesoporous Materials 108 (2008) 117-122.
[12] M. Konstantakou, A. Gotzias, M. Kainourgiakis, A.K. Stubos, T.A. Steriotis, GCMC simulations of gas adsorption in carbon pore structures, in: S. Mordechai (Ed.), Applications of Monte Carlo Method in Science and Engineering, InTech2011.
[13] A.D. Buckingham, R.L. Disch, D.A. Dunmur, Quadrupole moments of some simple molecules, Journal of the American Chemical Society 90 (1968) 3104-3107.
[14] C. Nguyen, D.D. Do, Adsorption of Supercritical Gases in Porous Media: Determination of Micropore Size Distribution, The Journal of Physical Chemistry B 103 (1999) 6900-6908.
[15] M. Lopez-Ramon, J. Jagiello, T. Bandosz, N. Seaton, Determination of the pore size distribution and network connectivity in microporous solids by adsorption measurements and Monte Carlo simulation, Langmuir : the ACS journal of surfaces and colloids 13 (1997) 4435-4445.
[16] J. Jagiello, C. Ania, J.B. Parra, C. Cook, Dual gas analysis of microporous carbons using 2D-NLDFT heterogeneous surface model and combined adsorption data of N2 and CO2, Carbon 91 (2015) 330-337.
[17] P. Tarazona, Free-energy density functional for hard spheres, Physical Review A 31 (1985) 2672-2679.
[18] P. Tarazona, Erratum: Free-energy density functional for hard spheres, Physical Review A 32 (1985) 3148-3148.
[19] R. Evans, U.M.B. Marconi, P. Tarazona, Fluids in narrow pores: Adsorption, capillary condensation, and critical points, The Journal of Chemical Physics 84 (1986) 2376-2399.
[20] C. Lastoskie, K.E. Gubbins, N. Quirke, Pore size distribution analysis of microporous carbons: a density functional theory approach, The Journal of Physical Chemistry 97 (1993) 4786-4796.
[21] J. Jagiello, J.P. Olivier, 2D-NLDFT adsorption models for carbon slit-shaped pores with surface energetical heterogeneity and geometrical corrugation, Carbon 55 (2013) 70-80.

[22] J. Jagiello, J.P. Olivier, Carbon slit pore model incorporating surface energetical heterogeneity and geometrical corrugation, Adsorption 19 (2013) 777-783.
[23] J.B. Parra, C.O. Ania, A. Arenillas, J.J. Pis, Textural characterisation of activated carbons obtained from poly(ethylene terephthalate) by carbon dioxide activation, in: B.M.J.R. F. Rodriguez-Reinoso, K. Unger (Eds.), Studies in Surface Science and Catalysis, Elsevier2002, pp. 537-543.
[24] J. Jagiello, J. Kenvin, A. Celzard, V. Fierro, Enhanced resolution of ultra micropore size determination of biochars and activated carbons by dual gas analysis using N2 and CO2 with 2D-NLDFT adsorption models, Carbon 144 (2019) 206-215.
[25] E.A. Ustinov, D.D. Do, V.B. Fenelonov, Pore size distribution analysis of activated carbons: Application of density functional theory using nongraphitized carbon black as a reference system, Carbon 44 (2006) 653-663.
[26] A.V. Neimark, Y. Lin, P.I. Ravikovitch, M. Thommes, Quenched solid density functional theory and pore size analysis of micro-mesoporous carbons, Carbon 47 (2009) 1617-1628.
[27] Q. Wang, J.K. Johnson, J.Q. Broughton, Path integral grand canonical Monte Carlo, The Journal of Chemical Physics 107 (1997) 5108.
[28] Q. Wang, J.K. Johnson, J. Broughton, Thermodynamic properties and phase equilibrium of fluid hydrogen from path integral simulations, Molecular Physics 89 (1996) 1105-1119.
[29] R.P. Feynman, A. Hibbs, Quantum Mechanics and Path Integrals, McGraw Hill, New York, 1965.
[30] L.M. Sesé, Study of the Feynman-Hibbs effective potential against the path-integral formalism for Monte Carlo simulations of quantum many-body Lennard-Jones systems, Molecular Physics 81 (1994) 1297-1312.
[31] W.A. Steele, The physical interaction of gases with crystalline solids: I. Gas-solid energies and properties of isolated adsorbed atoms, Surface Science 36 (1973) 317-352.
[32] P. Kowalczyk, R. Hołyst, A.P. Terzyk, P.A. Gauden, State of Hydrogen in Idealized Carbon Slitlike Nanopores at 77 K, Langmuir : the ACS journal of surfaces and colloids 22 (2006) 1970-1972.
[33] F. Darkrim, D. Levesque, Monte Carlo simulations of hydrogen adsorption in single-walled carbon nanotubes, The Journal of Chemical Physics 109 (1998) 4981-4984.
[34] P. Kowalczyk, P.A. Gauden, A.P. Terzyk, S.K. Bhatia, Thermodynamics of hydrogen adsorption in slit-like carbon nanopores at 77 K. Classical versus path-integral Monte Carlo simulations, Langmuir : the ACS journal of surfaces and colloids 23 (2007) 3666-3672.
[35] D.H. Everett, J.C. Powl, Adsorption in slit-like and cylindrical micropores in the henry's law region. A model for the microporosity of carbons, Journal of the Chemical Society, Faraday Transactions 1: Physical Chemistry in Condensed Phases 72 (1976) 619-636.
[36] J. Guo, J.R. Morris, Y. Ihm, C.I. Contescu, N.C. Gallego, G. Duscher, S.J. Pennycook, M.F. Chisholm, Topological defects: origin of nanopores and enhanced adsorption performance in nanoporous carbon, Small 8 (2012) 3283-3288.
[37] J. Jagiello, J. Kenvin, J. Olivier, A. Lupini, C. Contescu, Using a new finite slit pore model for NLDFT analysis of carbon pore structure, Adsorption Science & Technology 29 (2011) 769-780.
[38] B. Kuchta, L. Firlej, P. Pfeifer, C. Wexler, Numerical estimation of hydrogen storage limits in carbon-based nanospaces, Carbon 48 (2010) 223-231.
[39] P.I. Ravikovitch, A. Vishnyakov, R. Russo, A.V. Neimark, Unified Approach to Pore Size Characterization of Microporous Carbonaceous Materials from N2, Ar, and CO2 Adsorption Isotherms†, Langmuir : the ACS journal of surfaces and colloids 16 (2000) 2311-2320.
[40] J. Jagiello, C.O. Ania, J.B. Parra, L. Jagiello, J.J. Pis, Using DFT analysis of adsorption data of multiple gases including H2 for the comprehensive characterization of microporous carbons, Carbon 45 (2007) 1066-1071.
[41] M. Konstantakou, T.A. Steriotis, G.K. Papadopoulos, M. Kainourgiakis, E.S. Kikkinides, A.K. Stubos, Characterization of nanoporous carbons by combining CO2 and H2 sorption data with the Monte Carlo simulations, Applied Surface Science 253 (2007) 5715-5720.
[42] J. Jagiello, Stable numerical solution of the adsorption integral equation using splines, Langmuir : the ACS journal of surfaces and colloids 10 (1994) 2778-2785.

[43] J.T. Duda, L. Jagiełło, J. Jagiełło, J. Milewska-Duda, Complementary study of microporous adsorbents with DFT and LBET, Applied Surface Science 253 (2007) 5616-5621.
[44] P. Kleszyk, P. Ratajczak, P. Skowron, J. Jagiello, Q. Abbas, E. Frąckowiak, F. Béguin, Carbons with narrow pore size distribution prepared by simultaneous carbonization and self-activation of tobacco stems and their application to supercapacitors, Carbon 81 (2015) 148-157.
[45] G. Gregis, J.-B. Sanchez, S. Schaefer, V. Fierro, F. Berger, I. Bezverkhyy, G. Weber, J.-P. Bellat, A. Celzard, Detection of lung cancer bio-markers in human breath using a micro-fabricated air analyzer, Materials Today: Proceedings 2 (2015) 4664-4670.
[46] G. Gregis, S. Schaefer, J.-B. Sanchez, V. Fierro, F. Berger, I. Bezverkhyy, G. Weber, J.-P. Bellat, A. Celzard, Characterization of materials toward toluene traces detection for air quality monitoring and lung cancer diagnosis, Materials Chemistry and Physics 192 (2017) 374-382.
[47] D. Grau-Marin, J. Silvestre-Albero, E.O. Jardim, J. Jagiello, W.R. Betz, L.E. Peña, Evaluation of the textural properties of ultramicroporous carbons using experimental and theoretical methods, Carbon (2019). https://doi.org/10.1016/j.carbon.2019.10.035

Author contributions

Use this form to specify the contribution of each author of your manuscript. A distinction is made between five types of contributions: Conceived and designed the analysis; Collected the data; Contributed data or analysis tools; Performed the analysis; Wrote the paper.

For each author of your manuscript, please indicate the types of contributions the author has made. An author may have made more than one type of contribution. Optionally, for each contribution type, you may specify the contribution of an author in more detail by providing a one-sentence statement in which the contribution is summarized. In the case of an author who contributed to performing the analysis, the author's contribution for instance could be specified in more detail as 'Performed the computer simulations', 'Performed the statistical analysis', or 'Performed the text mining analysis'.

If an author has made a contribution that is not covered by the five pre-defined contribution types, then please choose 'Other contribution' and provide a one-sentence statement summarizing the author's contribution.

Manuscript title: Exploiting the adsorption of simple gases O2 and H2 with minimal quadrupole moments for the dual gas characterization of nanoporous carbons using 2D-NLDFT models

Author 1: Jacek Jagiello

☒ Conceived and designed the analysis
Specify contribution in more detail (optional; no more than one sentence)

☒ Collected the data
Specify contribution in more detail (optional; no more than one sentence)

☒ Contributed data or analysis tools
Specify contribution in more detail (optional; no more than one sentence)

☒ Performed the analysis
Specify contribution in more detail (optional; no more than one sentence)

☒ Wrote the paper
Specify contribution in more detail (optional; no more than one sentence)

☐ Other contribution
Specify contribution in more detail (required; no more than one sentence)

Author 2: Jeffrey Kenvin

☒ Conceived and designed the analysis
Specify contribution in more detail (optional; no more than one sentence)

☐ Collected the data
Specify contribution in more detail (optional; no more than one sentence)

☒ Contributed data or analysis tools
Specify contribution in more detail (optional; no more than one sentence)

☐ Performed the analysis
Specify contribution in more detail (optional; no more than one sentence)

☒ Wrote the paper
Contributed to writing the paper

☐ Other contribution
Specify contribution in more detail (required; no more than one sentence)

Author 3: Conchi O. Ania

☐ Conceived and designed the analysis
Specify contribution in more detail (optional; no more than one sentence)

☒ Collected the data
Specify contribution in more detail (optional; no more than one sentence)

☐ Contributed data or analysis tools
Specify contribution in more detail (optional; no more than one sentence)

☒ Performed the analysis
Specify contribution in more detail (optional; no more than one sentence)

☐ Wrote the paper
Specify contribution in more detail (optional; no more than one sentence)

☒ Other contribution
Synthetized the carbon samples

Author 4: Jose B. Parra

☐ Conceived and designed the analysis
Specify contribution in more detail (optional; no more than one sentence)

☒ Collected the data
Specify contribution in more detail (optional; no more than one sentence)

☐ Contributed data or analysis tools
Specify contribution in more detail (optional; no more than one sentence)

☒ Performed the analysis
Specify contribution in more detail (optional; no more than one sentence)

☐ Wrote the paper
Specify contribution in more detail (optional; no more than one sentence)

☒ Other contribution
Synthetized the carbon samples

Author 5: Alain Celzard

☒ Conceived and designed the analysis
Specify contribution in more detail (optional; no more than one sentence)

☒ Collected the data
Specify contribution in more detail (optional; no more than one sentence)

☒ Contributed data or analysis tools
Specify contribution in more detail (optional; no more than one sentence)

☐ Performed the analysis
Specify contribution in more detail (optional; no more than one sentence)

☐ Wrote the paper
Specify contribution in more detail (optional; no more than one sentence)

☐ Other contribution

Author 6: Vanessa Fierro

- ☒ Conceived and designed the analysis
  Specify contribution in more detail (optional; no more than one sentence)
- ☒ Collected the data
  Specify contribution in more detail (optional; no more than one sentence)
- ☐ Contributed data or analysis tools
  Specify contribution in more detail (optional; no more than one sentence)
- ☒ Performed the analysis
  Specify contribution in more detail (optional; no more than one sentence)
- ☐ Wrote the paper
  Specify contribution in more detail (optional; no more than one sentence)
- ☒ Other contribution
  Synthetized the carbon samples

Author 7: Enter author name

- ☐ Conceived and designed the analysis
  Specify contribution in more detail (optional; no more than one sentence)
- ☐ Collected the data
  Specify contribution in more detail (optional; no more than one sentence)
- ☐ Contributed data or analysis tools
  Specify contribution in more detail (optional; no more than one sentence)
- ☐ Performed the analysis
  Specify contribution in more detail (optional; no more than one sentence)
- ☐ Wrote the paper
  Specify contribution in more detail (optional; no more than one sentence)
- ☐ Other contribution
  Specify contribution in more detail (required; no more than one sentence)

Author 8: Enter author name

- ☐ Conceived and designed the analysis
  Specify contribution in more detail (optional; no more than one sentence)
- ☐ Collected the data
  Specify contribution in more detail (optional; no more than one sentence)
- ☐ Contributed data or analysis tools
  Specify contribution in more detail (optional; no more than one sentence)
- ☐ Performed the analysis
  Specify contribution in more detail (optional; no more than one sentence)
- ☐ Wrote the paper
  Specify contribution in more detail (optional; no more than one sentence)
- ☐ Other contribution
  Specify contribution in more detail (required; no more than one sentence)

Author 9: Enter author name

- ☐ Conceived and designed the analysis
  Specify contribution in more detail (optional; no more than one sentence)
- ☐ Collected the data
  Specify contribution in more detail (optional; no more than one sentence)
- ☐ Contributed data or analysis tools
  Specify contribution in more detail (optional; no more than one sentence)
- ☐ Performed the analysis
  Specify contribution in more detail (optional; no more than one sentence)
- ☐ Wrote the paper
  Specify contribution in more detail (optional; no more than one sentence)
- ☐ Other contribution
  Specify contribution in more detail (required; no more than one sentence)

Author 10: Enter author name

- ☐ Conceived and designed the analysis
  Specify contribution in more detail (optional; no more than one sentence)
- ☐ Collected the data
  Specify contribution in more detail (optional; no more than one sentence)
- ☐ Contributed data or analysis tools
  Specify contribution in more detail (optional; no more than one sentence)
- ☐ Performed the analysis
  Specify contribution in more detail (optional; no more than one sentence)
- ☐ Wrote the paper
  Specify contribution in more detail (optional; no more than one sentence)
- ☐ Other contribution
  Specify contribution in more detail (required; no more than one sentence)

Declaration of interests

☒ The authors declare that they have no known competing financial interests or personal relationships that could have appeared to influence the work reported in this paper.

☐The authors declare the following financial interests/personal relationships which may be considered as potential competing interests:

No financial support was received for this work.